

## Giant Spin Splitting through Surface Alloying

Christian R. Ast,<sup>1,2,\*</sup> Jürgen Henk,<sup>3</sup> Arthur Ernst,<sup>3</sup> Luca Moreschini,<sup>2</sup> Mihaela C. Falub,<sup>2</sup> Daniela Pacil ,<sup>2,†</sup>  
Patrick Bruno,<sup>3</sup> Klaus Kern,<sup>1,2</sup> and Marco Grioni<sup>2</sup>

<sup>1</sup>Max-Planck-Institut f r Festk rperforschung, D-70569 Stuttgart, Germany

<sup>2</sup>Ecole Polytechnique F d rale de Lausanne (EPFL), Institut de Physique des Nanostructures, CH-1015 Lausanne, Switzerland

<sup>3</sup>Max-Planck-Institut f r Mikrostrukturphysik, D-06120 Halle (Saale), Germany

(Received 26 October 2006; published 3 May 2007)

The long-range ordered surface alloy Bi/Ag(111) is found to exhibit a giant spin splitting of its surface electronic structure due to spin-orbit coupling, as is determined by angle-resolved photoelectron spectroscopy. First-principles electronic structure calculations fully confirm the experimental findings. The effect is brought about by a strong in-plane gradient of the crystal potential in the surface layer, in interplay with the structural asymmetry due to the surface-potential barrier. As a result, the spin polarization of the surface states is considerably rotated out of the surface plane.

DOI: 10.1103/PhysRevLett.98.186807

PACS numbers: 73.20.At, 71.70.Ej, 79.60.-i

In nonmagnetic solids, electronic states of opposite spin orientation are often implicitly taken to be degenerate (Kramers' degeneracy). However, spin degeneracy is a consequence of both time-reversal and inversion symmetry. If one of the latter is broken, the degeneracy can be lifted by, e.g., the spin-orbit (SO) interaction. This is, for example, the case in crystals that lack a center of inversion in the bulk (Dresselhaus effect) [1,2]. But also a structural inversion asymmetry, as it shows up at surfaces or interfaces, can lead to spin-split electronic states [Rashba-Bychkov (RB) effect] [3]. In particular, clean surfaces of noble metals show spin-split surface states, where the splitting increases with the strength of the atomic SO coupling (cf. Ag and Au in Table I). The splitting can be further enhanced by adsorption of adatoms [9–12]. Hence, using morphology and chemistry to tune the spin splitting of two-dimensional electronic states is a promising path to create a new class of nanoscale structures suitable for spintronic devices. Doping GaAs by only a few percent with Bi atoms has been shown to strongly increase the spin-orbit splitting energy  $\Delta_0$  [13]. However, a value for the Rashba-Bychkov type spin splitting has not been reported.

The Au(111)  $L$ -gap surface state is the paradigm of a Rashba-Bychkov system with a spin splitting of a few tens of meV, that was investigated in detail by means of spin- and angle-resolved photoelectron spectroscopy (ARPES) [14]. The nonrelativistic Hamilton operator of the spin-orbit interaction,

$$\hat{H}_{\text{SO}} \propto \frac{\hbar^2}{2m^2c^2} \boldsymbol{\sigma} \cdot (\nabla V \times \hat{\mathbf{p}}), \quad (1)$$

can be expressed for a two-dimensional gas of free electrons (in the  $xy$  plane) as

$$\hat{H}_{\text{SO}} = \alpha_R \boldsymbol{\sigma} \cdot (\mathbf{k}_{\parallel} \times \mathbf{e}_z), \quad (2)$$

in which the Rashba parameter  $\alpha_R$  is essentially determined by the gradient of the potential  $V$  in  $z$  direction,  $\alpha_R \propto \partial V / \partial z$ .  $\hbar \mathbf{k}_{\parallel} = \hbar(k_x, k_y)$  is the in-plane momentum,

and  $\boldsymbol{\sigma}$  is the vector of Pauli matrices. This model reproduces remarkably well the very characteristic dispersion of the spin-split surface-state bands of Au(111). The spin polarizations  $\mathbf{P}$  of the split and completely polarized ( $|\mathbf{P}| = 100\%$ ) electronic states lie axially symmetric within the surface plane ( $\mathbf{P} \perp \mathbf{k}_{\parallel} \perp \mathbf{e}_z$ ). Time-reversal symmetry requires  $\mathbf{P}(\mathbf{k}_{\parallel}) = -\mathbf{P}(-\mathbf{k}_{\parallel})$  and  $E(\mathbf{k}_{\parallel}) = E(-\mathbf{k}_{\parallel})$ .

The two main contributions to the spin splitting are a strong atomic SO interaction and a potential gradient along the surface normal ( $z$  direction). By adsorption of noble gases and oxygen, the spin splitting was successfully enhanced by increasing the surface-potential gradient [9,12]. However, changing the in-plane potential gradient has not been reported so far. Surface alloying, in particular, provides interesting opportunities as the adatoms replace atoms of the clean surface layer. This would alter the hybridization of electronic states within that layer and thereby create a new two-dimensional (2D) electronic structure. Prerequisites for a sizable effect are (i) a long-range ordered surface alloy to maintain 2D electronic states and (ii) comparably light atoms surrounding heavy atoms. From such a configuration we would expect a large in-plane potential gradient and consequently a giant splitting accompanied by a large  $P_z$  component [see Eq. (1)].

In this Letter we report on a new class of materials that exhibits a giant spin splitting in the surface electronic

TABLE I. Selected materials and parameters characterizing the spin splitting: Rashba energy of split states  $E_R$ , wave number offset  $k_0$ , and Rashba parameter  $\alpha_R$ .

Material	$E_R$ (meV)	$k_0$ ( $\text{\AA}^{-1}$ )	$\alpha_R$ (eV $\text{\AA}$ )	Reference
InGaAs/InAlAs heterostructure	<1	0.028	0.07	[4]
Ag(111) surface state	<0.2	0.004	0.03	[5,6]
Au(111) surface state	2.1	0.012	0.33	[6,7]
Bi(111) surface state	~14	~0.05	~0.56	[8]
Bi/Ag(111) surface alloy	200	0.13	3.05	This work

structure. Using the concept of surface alloying, the Ag(111) ( $Z = 47$ ) surface layer was doped with the heavy element Bi ( $Z = 83$ ). The 2D band structure of the Bi/Ag(111) surface alloy was investigated by ARPES [at the EPFL in Lausanne, Switzerland, as well as at the Synchrotron Radiation Center (SRC) in Wisconsin, U.S.A.] and exhibits a spin splitting of unprecedented magnitude. We have shown elsewhere [15] that the large spin-orbit splitting opens up new opportunities for STM investigation of SO split states. Here we focus on the electronic structure of the surface alloy, and provide a theoretical explanation for the effect by means of first-principles electronic structure calculations. The sizable spin splitting is explained by the in-plane potential gradient.

The Ag(111) surface was cleaned in ultrahigh vacuum using successive sputtering and annealing cycles. The deposition of 1/3 of a monolayer of Bi atoms results in a long-range ordered ( $\sqrt{3} \times \sqrt{3}$ ) $R30^\circ$  substitutional surface alloy [see Fig. 1(a)]. The Bi atoms protrude slightly out of the surface due to size mismatch [Fig. 1(b)] [15]. A similar scenario is observed for the Sb/Ag(111) surface alloy [16].

The experimental electronic structure of Bi/Ag(111) [Fig. 1(c)] consists of one pair of bands that shows strong photoemission intensity (dark) at the maxima ( $-0.135$  eV), which becomes weaker (lighter) with increasing binding energy [17]. The maxima are symmetrically shifted from the  $\bar{\Gamma}$  point by  $0.13 \text{ \AA}^{-1}$ ; the effective mass  $m^*$  is  $-0.35m_e$ . A second pair with much less intensity crosses the Fermi level at positions indicated by the four arrows in Fig. 1(c). The separation between these bands is  $0.12 \text{ \AA}^{-1}$ .

The above findings—a symmetric offset of band extrema [Bi/Ag(111): maxima; Au(111): minima] in conjunction with a crossing at  $\bar{\Gamma}$ —clearly indicate a spin-split

surface band structure due to spin-orbit interaction, as in the RB model and for Au(111). However, the splitting is considerably larger than those reported for other systems [9–12,18]. Different splittings can be compared on a wave number scale, where  $k_0$  describes the shift of the band extremum away from  $\bar{\Gamma}$  as well as on an energy scale, where  $E_R = \hbar^2 k_0^2 / 2m^*$  is called Rashba energy [see Fig. 1(c)]. If there were no spin splitting the dispersion would reduce to a spin-degenerate band with the maximum at the high symmetry point. The Rashba parameter  $\alpha_R = \hbar^2 k_0 / m^*$  is the coupling constant in the spin-orbit Hamiltonian [Eq. (2)]. A selection of systems is given in Table I, where the Rashba parameter has been computed from the experimentally accessible quantities  $k_0$  and  $m^*$ .

In the following we argue that the RB model, as given by Eq. (2), cannot explain our findings for a surface alloy. It was shown that the Rashba parameter  $\alpha_R$  of the  $L$ -gap surface state of a  $\text{Ag}_x\text{Au}_{1-x}$  alloy depends linearly on the concentration  $x$ , as in the virtual crystal approximation [6]. Hence, one is tempted to conclude that  $\alpha_R$  is essentially determined by the number of heavy atoms (here Au,  $Z = 79$ ) probed by the surface state. If one were to apply the same idea to Bi/Ag(111), with Bi being the heavy element ( $Z = 83$ ), one would expect  $\alpha_R$  to be about an order of magnitude smaller ( $0.3$  to  $0.4 \text{ eV \AA}$ ) than what was found experimentally (see Table I). The potential gradient along the  $z$  direction is expected almost independent of the specific surface, and a strong atomic SO interaction alone cannot account for our findings. Hence, there must be an additional mechanism responsible for the observed giant splitting.

The electronic structure of the Bi/Ag(111) surface alloy was calculated from first principles within the framework of the local spin-density approximation to density-functional theory (DFT). A relativistic multiple-scattering approach (layer Korringa-Kohn-Rostoker method), in which spin-orbit coupling is fully accounted for (Dirac equation), was used to compute spin-, layer-, and atom-resolved Bloch spectral densities, hence allowing one to characterize the electronic structure in much detail. Its suitability for investigating RB systems was already proven for the  $L$ -gap surface state of Au(111) [19]. Calculations for the clean Ag(111) surface agree well with experiment. In the theory, the SO interaction can be scaled between the fully relativistic (Dirac equation) and the scalar-relativistic case [20,21]. In the latter case (not shown), the spin splitting vanishes. This clearly proves that SO coupling is the base of the observed effect.

A first comparison of experiment and theory is done by considering  $I(E; k_x, k_y)$  slices, where  $I$  is either the experimental photoemission intensity or the theoretical Bloch spectral density of the surface layer (cf. Ref. [15]).  $I$  is shown in Fig. 2 as gray scale for fixed  $k_y$  (along  $\bar{\Gamma}-\bar{K}$ ) and varying both energy  $E$  and  $k_x$  (along  $\bar{M}-\bar{\Gamma}-\bar{M}$ ). For  $k_y = 0$  [Fig. 2(a)], both experiment (left-hand panels) and theory (right-hand panels) exhibit the characteristic dispersion of

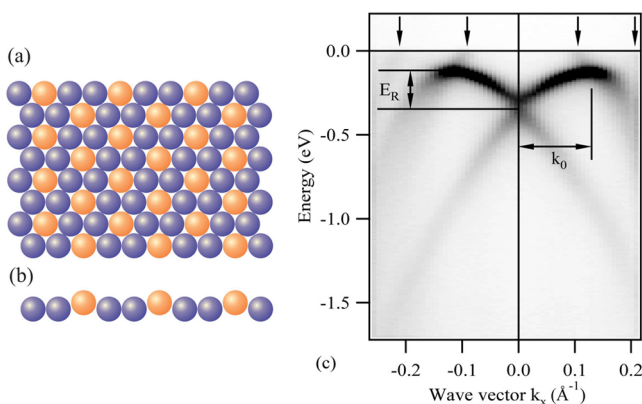


FIG. 1 (color online). (a) Schematic top view of the ( $\sqrt{3} \times \sqrt{3}$ ) $R30^\circ$  Bi/Ag(111) surface alloy [Bi, light gray (orange); Ag, dark gray (blue)]. (b) Side view of the schematic, illustrating the outward relaxation of Bi in the surface layer. (c) Experimental band structure obtained by ARPES. The abscissa is the wave vector  $k_x$  along the  $\bar{M}-\bar{\Gamma}-\bar{M}$  line in the vicinity of the center of the surface alloy Brillouin zone ( $\bar{\Gamma}$ , i.e.,  $k_{\parallel} = 0$ ). The ordinate gives the energy below the Fermi level (0 eV).

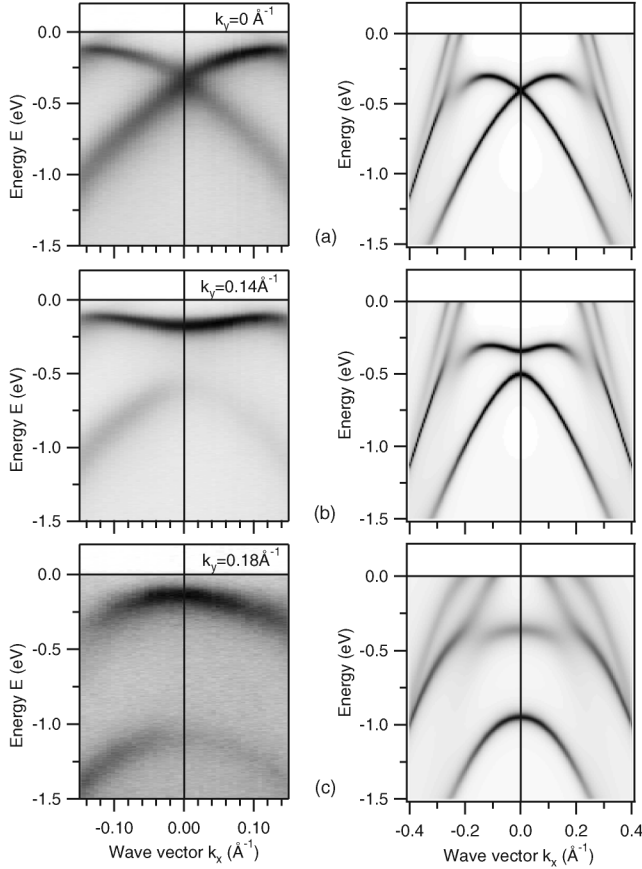


FIG. 2. Band structure measurements by ARPES (left-hand panels) and calculations (right-hand panels) in the vicinity of the  $\bar{\Gamma}$  point. Note the different horizontal scales.

the first and second pair of RB-split bands. The experimental splitting of  $k_0 = 0.13 \text{ \AA}^{-1}$  in the first set of bands is well reproduced by the calculations. The effective mass of the first band pair is somewhat higher in theory ( $-0.63m_e$ ) than in experiment. Furthermore, the crossing at  $\bar{\Gamma}$  is lower in energy than in experiment by about 0.1 eV, possibly due to an underestimation of the outward Bi relaxation [ $\Delta z = 0.35 \text{ \AA}$ , Fig. 1(b)].

Figure 2(a) (right-hand panel) shows that the first band pair (mainly of  $sp_z$  character) hybridizes with the second pair ( $p_x p_y$  states). This is evident from the weak Bloch spectral density around ( $E = -0.4 \text{ eV}$ ,  $k_x = \pm 0.2 \text{ \AA}^{-1}$ ). The crossing area shows up at larger  $|k_x|$  than in experiment. The electronic states of both band pairs are strongly localized within the surface layer, in contrast to Au(111), for which the  $L$ -gap surface state is transversally extended over several layers [22,23]. For increasing  $k_y$  [Figs. 2(b) and 2(c)] the agreement of experiment (left-hand panels) and theory (right-hand panels) is maintained.

A hint on the new mechanism for the giant splitting is provided by momentum distributions (MD), i.e., for  $I(E; k_x, k_y)$  slices for fixed energy  $E$ . The experimental momentum distribution for  $E = -0.17 \text{ eV}$ , shown as gray scale in Fig. 3(d), displays four contours (C1 to C4),

which are indicated by arrows. The intensity scale is logarithmic to enhance the weaker features in the image. The contours C1 + C2 and C3 + C4 correspond to the first and second set of bands, respectively. Note that the contours C2 and C3 are the overlapping bands in Fig. 1(c). The contours C1 and C3 at small  $|k_{\parallel}|$  are circular, while the contours C2 and C4 at larger  $|k_{\parallel}|$  have hexagonal shape. Hence, we find a significant deviation of the MD from the circular shape in the RB model [cf. Refs. [7,19,24] for Au(111)]. A hexagonal MD is characteristic for the associated electrons being subject to the crystal potential [with point group  $3m$  for Bi/Ag(111)].

The crystal potential  $V$  directly influences the spin polarization of the electrons, as is evident from the expression for the SO interaction, Eq. (1). The potential gradient in the  $z$  direction results in an in-plane spin polarization, as in the RB model, Eq. (2). An in-plane gradient, however, leads to a nonzero  $P_z$ . Conversely, a sizable  $P_z$  indicates a significant in-plane gradient of  $V$ . A closer analysis within a 2D nearly free electron (NFE) model shows further that the effect on  $P_z$  increases with  $|k_{\parallel}|$  [25].

The computed spin polarization at the momentum distributions with (almost) circular shape [black lines in Figs. 3(a)–3(c)] lies mainly within the surface plane and shows the typical behavior of the RB model. Close to  $\bar{\Gamma}$ ,  $P_z$

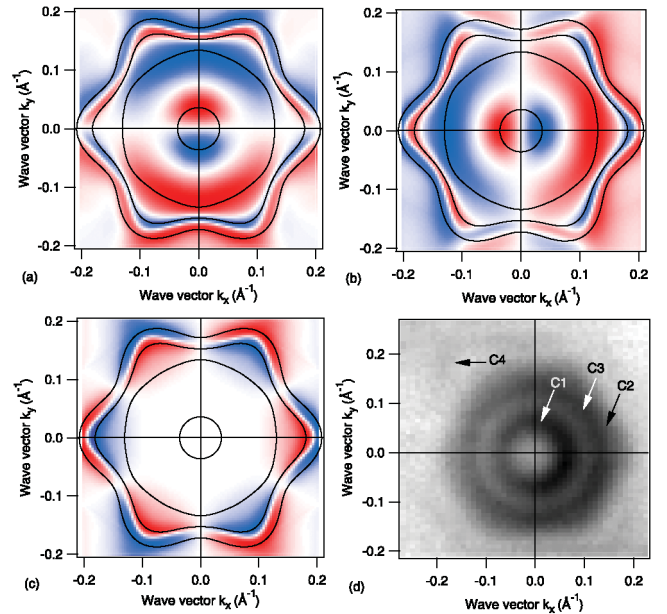


FIG. 3 (color). (a)–(c) Constant energy contour of the spin polarization  $\mathbf{P}$  in  $x$ ,  $y$ , and  $z$  direction, respectively, at an energy of  $-0.55 \text{ eV}$ . The projection in  $x$ ,  $y$ , and  $z$  direction is shown in (a)–(c), respectively. The intensity scale is linear with red and blue coloring corresponding to positive and negative values, respectively. White areas indicate sign changes, where the projection is zero. The constant energy contours of the band dispersion are shown as black lines, where the two inner contours correspond to the first set of bands in Fig. 1(c), while the two outer contours correspond to the second set of bands. (d) Constant energy map by ARPES at an energy of  $-0.17 \text{ eV}$ .

is close to zero [Fig. 3(c)], establishing  $\mathbf{P} \perp \mathbf{k}_{\parallel} \perp \mathbf{e}_z$  in very good approximation. With increasing  $|\mathbf{k}_{\parallel}|$  the contours deviate from the circular shape and  $P_z$  becomes as large as 10% (in absolute value), indicating a substantial out-of-plane rotation of  $\mathbf{P}$ . Correspondingly, the in-plane  $\mathbf{P}$  components ( $\mathbf{P}_{\parallel}$ ) are less than 80%. For the RB paradigm Au(111), 1.4% and 97% for  $P_z$  and  $|\mathbf{P}_{\parallel}|$ , respectively, were found [19].

The first-principles calculations do not allow one to separate directly the different contributions to the spin splitting, in contrast to a NFE model for a 2D electron gas [25]. The NFE calculations fully confirm the findings of the *ab initio* calculations and show further that the in-plane potential gradient contributes considerably to the strength of the spin splitting. We conclude that the giant spin splitting in the Bi/Ag(111) surface alloy is the result of a strong in-plane potential gradient.

The Bi/Ag(111) surface alloy is the first system for which a giant spin splitting is observed. It goes beyond the giant spin-orbit bowing effect seen in the doped GaAs<sub>1-x</sub>Bi<sub>x</sub> system [13], since here the spin splitting is manipulated directly through the in-plane gradient. This gradient has its origin in the concept of surface alloying itself: each Bi atom is surrounded by six Ag atoms, which results in a strong in-plane gradient of the potential, possibly enhanced further by the outward relaxation of the Bi atom. The threefold rotational symmetry of the surface destroys the inversion symmetry within the surface plane. The DFT calculations show that the electronic surface states are strongly localized within the topmost surface layer, exposing them substantially to the in-plane gradient.

In conclusion, we have identified the Bi/Ag(111) surface alloy as a member of a new class of materials for which a strong spin splitting is observed. The spin splitting results from a sizable in-plane gradient of the potential that contributes to the splitting strength. The in-plane gradient manifests itself in the out-of-plane rotation of the spin polarization, as obtained from first-principles calculations, as well as in a hexagonal shape of the outer branches in the constant energy contours. Spin-resolved photoemission measurements are in preparation to experimentally confirm the out-of-plane rotation of the spin. This mechanism opens up a new degree of freedom for manipulating the spin-orbit splitting of two-dimensional electronic states.

We gratefully acknowledge H. Höchst, R. Hatch, S. Gorovikov, and M. Papagno for help with the experiments, as well as P. Wahl, M. Trautmann, J. Premper, and S. Blügel for stimulating discussions. Part of this work has been done at the SRC (University of Wisconsin–Madison), which is funded by the NSF under Grant No. DMR-0537588. The work at the EPFL has been supported by the Swiss National Science Foundation and NCCR MaNEP.

\*Corresponding author.

Email address: c.ast@fkf.mpg.de

†Permanent address: INFN and Università degli studi della Calabria, 87036 Rende, Cosenza, Italy.

- [1] G. Dresselhaus, Phys. Rev. **100**, 580 (1955).
- [2] J. Königmann, R. J. Haug, D. K. Maude, V. I. Fal'ko, and B. L. Altshuler, Phys. Rev. Lett. **94**, 226404 (2005).
- [3] Y. A. Bychkov and E. I. Rashba, JETP Lett. **39**, 78 (1984).
- [4] J. Nitta, T. Akazaki, H. Takayanagi, and T. Enoki, Phys. Rev. Lett. **78**, 1335 (1997).
- [5] D. Popović, F. Reinert, S. Hüfner, V. G. Grigoryan, M. Springborg, H. Cercellier, Y. Fagot-Revurat, B. Kierren, and D. Malterre, Phys. Rev. B **72**, 045419 (2005).
- [6] H. Cercellier, C. Didiot, Y. Fagot-Revurat, B. Kierren, L. Moreau, D. Malterre, and F. Reinert, Phys. Rev. B **73**, 195413 (2006).
- [7] S. LaShell, B. A. McDougall, and E. Jensen, Phys. Rev. Lett. **77**, 3419 (1996).
- [8] Y. M. Koroteev, G. Bihlmayer, J. E. Gayone, E. V. Chulkov, S. Blügel, P. M. Echenique, and P. Hofmann, Phys. Rev. Lett. **93**, 046403 (2004).
- [9] F. Forster, S. Hüfner, and F. Reinert, J. Phys. Chem. B **108**, 14692 (2004).
- [10] E. Rotenberg, J. W. Chung, and S. D. Kevan, Phys. Rev. Lett. **82**, 4066 (1999).
- [11] M. Hochstrasser, J. G. Tobin, E. Rotenberg, and S. D. Kevan, Phys. Rev. Lett. **89**, 216802 (2002).
- [12] O. Krupin, G. Bihlmayer, K. Starke, S. Gorovikov, J. E. Prieto, K. Döbrich, S. Blügel, and G. Kaindl, Phys. Rev. B **71**, 201403(R) (2005).
- [13] B. Fluegel, S. Francoeur, A. Mascarenhas, S. Tixier, E. C. Young, and T. Tiedje, Phys. Rev. Lett. **97**, 067205 (2006).
- [14] M. Hoesch, M. Muntwiler, V. N. Petrov, M. Hengsberger, L. Patthey, M. Shi, M. Falub, T. Greber, and J. Osterwalder, Phys. Rev. B **69**, 241401(R) (2004).
- [15] C. R. Ast, D. Pacilé, M. Falub, L. Moreschini, M. Papagno, G. Wittich, P. Wahl, R. Vogelgesang, M. Grioni, and K. Kern, cond-mat/0509509.
- [16] E. A. Soares, C. Bittencourt, V. B. Nascimento, V. E. de Carvalho, C. M. C. de Castilho, C. F. McConville, A. V. de Carvalho, and D. P. Woodruff, Phys. Rev. B **61**, 13983 (2000).
- [17] The measurements were done at 25 K using 29 eV photons in ultrahigh vacuum ( $2 \times 10^{-10}$  mbar). The energy and momentum resolution of the analyzer were better than 10 meV and  $\pm 0.015 \text{ \AA}^{-1}$ . Samples were prepared *in situ*.
- [18] K. Sugawara, T. Sato, S. Souma, T. Takahashi, M. Arai, and T. Sasaki, Phys. Rev. Lett. **96**, 046411 (2006).
- [19] J. Henk, M. Hoesch, J. Osterwalder, A. Ernst, and P. Bruno, J. Phys. Condens. Matter **16**, 7581 (2004).
- [20] H. Ebert, H. Freyer, and M. Deng, Phys. Rev. B **56**, 9454 (1997).
- [21] E. Tamura (private communication).
- [22] J. Henk, A. Ernst, and P. Bruno, Phys. Rev. B **68**, 165416 (2003).
- [23] J. Henk, A. Ernst, and P. Bruno, Surf. Sci. **566–568**, 482 (2004).
- [24] F. Reinert, J. Phys. Condens. Matter **15**, S693 (2003).
- [25] M. Trautmann, J. Premper, J. Henk, and P. Bruno (to be published).